Supporting Information

Biophysical characterization of supported lipid bilayers using parallel dual-wavelength surface plasmon resonance and quartz crystal microbalance measurements

Petteri Parkkila[1,*], Mohamed Elderdfi[2], Alex Bunker[1] and Tapani Viitala[1]

[1] Drug Research Program, Division of Pharmaceutical Biosciences, Faculty of Pharmacy, University of Helsinki, 00014 Helsinki, Finland

[2] Department of Cytobiochemistry, Faculty of Biotechnology, University of Wrocław, 50-383 Wrocław, Poland

* Corresponding author information: e-mail: petteri.parkkila@helsinki.fi , tel: +358 50 4655801

Address: Viikinkaari 5 E, P.O.Box 56, 00014 University of Helsinki, Finland

Table of Contents

Definition of the error parameters

Error values of different parameters in the study using three independent measurements are calculated as standard errors of the mean, defined as

$$S.E.M = \frac{s}{\sqrt{N}}, \tag{S1}$$

where N is the number of experiments and s is the standard deviation,

$$s = \sqrt{\frac{\sum_{i=1}^{N}(x_i - \bar{x})^2}{N-1}}. \tag{S2}$$

In the equation, x_i are the measured experimental or calculated values, and $\bar{x}$ is the mean of N values.

Size distributions of the vesicles

Table S1: Average size distributions of vesicles measured with dynamic light scattering. Values are averaged from three consequent measurements

	Average Vesicle Diameter (nm)	Polydispersity Index
DOPC	65.99 ± 18.83	0.145 ± 0.040
DOPC-DOPS (7:3 molar ratio)	63.20 ± 17.67	0.110 ± 0.006
POPC	64.85 ± 17.58	0.167 ± 0.008
DOPC-Sm-Chol (1:1:1 molar ratio)	60.38 ± 6.07	0.144 ± 0.016
DPPC	56.66 ± 14.24	0.328 ± 0.013

Calculation of SPR sensor parameters

Layer parameters of different SPR sensor slides were fitted by using Simulation mode 3 in the LayerSolver™ software (Figure S1). Thicknesses of the gold and chromium layers were set as dependent variables (D) between the two wavelengths while the refractive indices were set as independent variables (V). SiO_2 layer thickness was set as a dependent parameter (D) and refractive indices were fixed (F). Initial refractive indices of the bulk medium were calculated from the angles of total internal reflection provided by the data collection software and were kept as fixed parameters (F). After the parameters of each sensor slide were calculated, the properties of the formed layers were analyzed (see next sections). Optical parameters for one SiO_2 sensor are presented in Table S2.

In order to calculate the bulk sensitivity parameter, S (used in eq 4 in the main text) for the silica sensors, HEPES-NaCl buffer was injected in series with different HEPES concentrations (20, 40, 60, 80, 100 mM). Sensitivity parameters for the two wavelengths of 670 nm and 785 nm were then defined as S = Δ SPR angle/Δ Refractive index of the bulk. Bulk refractive indices were calculated from the angle of total internal reflection using Snell's law.

Table S2: Optical parameters used in the SPR modeling for one SiO_2 sensor.

Layer	Thickness, $\boldsymbol{d}$ (nm)	Real part of the refractive index, $\boldsymbol{n}$ (670 nm)	Imaginary part of the refractive index, $\boldsymbol{k}$ (670 nm)	Real part of the refractive index, $\boldsymbol{n}$ (785 nm)	Imaginary part of the refractive index, $\boldsymbol{k}$ (785 nm)
Glass	Infinite	1.52180 (F)	0 (F)	1.51760 (F)	0 (F)
Chromium	7.86 (D)	4.17635 (V)	0.06338 (V)	4.74171 (V)	0.03417 (V)
Gold	50.99 (D)	0.23449 (V)	4.22160 (V)	0.21964 (V)	5.32671 (V)
SiO_2	20.01 (D)	1.47200 (F)	0 (F)	1.47030 (F)	0 (F)
Buffer	Infinite	1.33265 (F)	0 (F)	1.33005 (F)	0 (F)

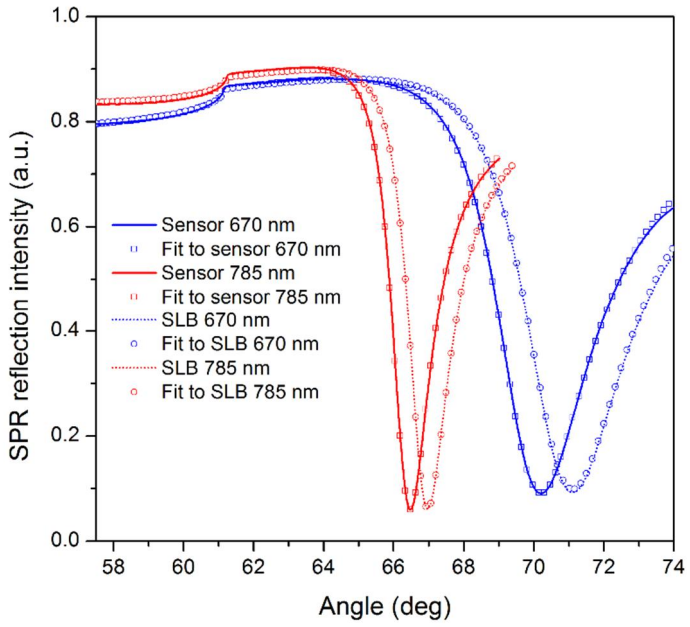

Figure S1: SPR reflection spectra and corresponding fits of the Fresnel multi-layer equations.

Inverse dual-wavelength analysis

Since the inverse dispersion coefficient analysis is not implemented in the LayerSolver™ software, the analysis has to be performed manually. For SLBs investigated in this study, the procedure was as follows:

1) Calculate the bulk refractive indices from the angle of total internal reflection using Snell's law and use these values as the model values for the bulk refractive indices.
2) Calculate the layer parameters of the SiO_2 sensor using Simulation mode 3 as detailed in the previous section.
3) Using the obtained layer parameters as fixed values, add another layer corresponding to the lipid bilayer, and model the reflection spectra obtained for a time-point after the SLB has been formed.
4) Set the thickness of the bilayer as a fixed value (F, same value for the both wavelengths) and refractive index as a variable (V) for both wavelengths.
5) Run the simulation engine for different values of layer thickness (3, 4, 5 and 6 nm, for example) and collect the refractive index values n_1 and n_2 for each value of the modeled thickness.

6) Calculate dispersion coefficients (eq 1 in the main text) for each value of modeled thickness and plot the dispersion coefficient as a function of the modeled thickness. If no minimum is formed, adjust $n_{b,2}$ and repeat step 5. Please note that, in this case, only the re-calculation of n_2 values are needed.

Figure S2A shows the change in thickness value corresponding to the dispersion coefficient minimum as a function of the refractive index of the second wavelength for one particular experiment involving a DOPC bilayer. As highlighted with the dotted circle, there are two possible values that could be selected. The origin of the kink, or deflection, in the data plot is not known, but it may be due to the software starting to treat the adlayer as a thin optical film. Closer inspection of the data (Figure S2B) shows that the width of the peak minimum is not as narrow at $n_{b,2}$ = 1.32936 (width of the minimum 0.7 nm) as it is at $n_{b,2}$ = 1.32937 (0.4 nm). Thus, the latter was selected.

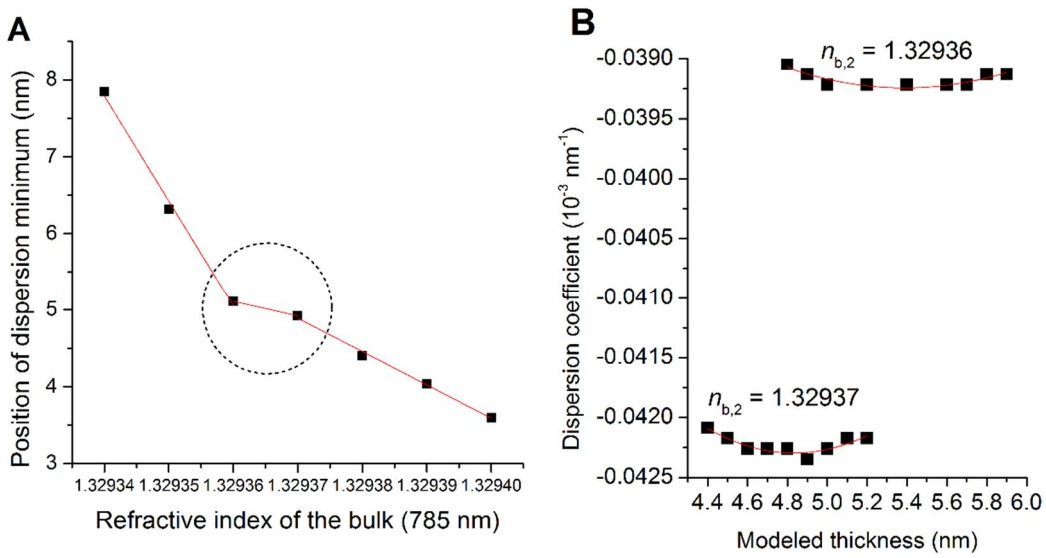

Figure S2: A) Model thickness value of the bilayer at different refractive indices of the bulk liquid. B) Closer inspection of the dispersion coefficient minima reveals that the peak minimum width is higher with the lower value of $n_{b,2}$.

SPR experimental details

Hydration-layer analysis was performed by using parameters presented in Table S3. Refractive indices of the water layer were chosen as $n_{b,1}$ = 1.32965 and $n_{b,2}$ = 1.32734. The initial values of the fits for the layer formation analysis are presented in Table S4 (Simulation modes 2 and 3 of the LayerSolver™ software were used for determining each initial value). Respective SPR sensorgrams are presented in Figure S3. For the DOPC-Sm-Chol mixture, an additional step of injection of ultrapure H_2O was added subsequent to the vesicle injection to ensure complete SLB formation, although this had no significant effect on the final values of SPR peak angle minimum.

Table S3: Molecular weight, molar refractivity, ratio of molar refractivity and molecular weight, and anisotropy values for different lipids and lipid compositions used in the calculations. Molecular weight and molar refractivity values were derived from the LIPID Metabolites and Pathways Strategy (LIPID MAPS) website[1], and anisotropy values were obtained from the study of Mashaghi et al.[2]

	$\boldsymbol{M}$ (g/mol)	$\boldsymbol{A}$ (mL/mol)	$\boldsymbol{r}$ (mL/g)	$\boldsymbol{\phi}$
DOPC	785.5935	224.62	0.2859	0.0139
DOPS	810.5256	219.44	0.2707	-
POPC	759.5778	215.48	0.2837	0.0196
Sphingomyelin	650.697	184.90	0.2840	-
Cholesterol	386.650	119.56	0.3092	-
DOPC-DOPS	793.0731[a]	-	0.2814[a]	0.0250
DOPC-Sm-Chol	607.3021[a]	-	0.2927[a]	0.0200[b]
DPPC	733.5622	206.34	0.2813	0.0200[b]

[a] calculated as molar-fraction-weighted-averages

[b] an estimate for lipid bilayer anisotropy was used for DOPC-Sm-Chol and DPPC

Table S4: Initial values used for layer analysis for each time-point (presented in Figure S4A) during the SLB formation process. The initial value for the dispersion coefficient was kept as constant, $dn/d\lambda$ = -0.035 · 10^{-3} nm^{-1}.

	SLBs		DPPC vesicles	
Time-point #	$\boldsymbol{d}$ (nm)	$\boldsymbol{n_1}$	$\boldsymbol{d}$ (nm)	$\boldsymbol{n_1}$
1	5 10	1.35 1.35	20 40	1.35 1.35
2	5 10 20	1.35 1.35 1.35	20 40	1.35 1.35
3	5 10	1.40 1.40	40 60	1.35 1.35
4	5 10	1.40 1.40	40 60	1.35 1.35
5	5 10	1.48 1.40	40 60	1.35 1.35
6	5 6	1.48 1.48	40 60	1.35 1.35

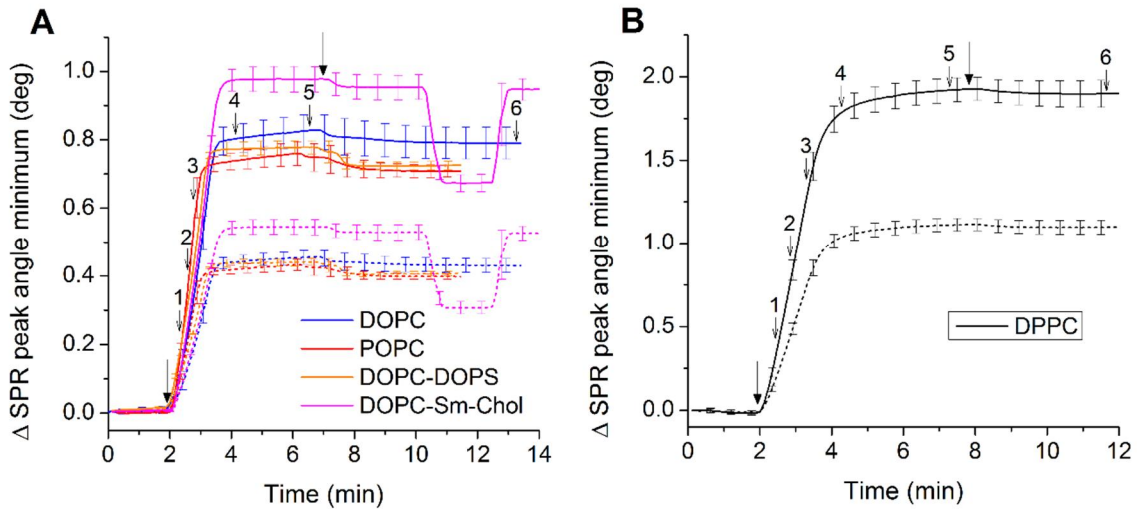

Figure S3: SPR sensorgrams for 670 nm (solid lines) and 785 nm (dashed lines) wavelengths for A) SLB-forming vesicles and B) DPPC vesicles forming SVLs. The short arrows indicate the approximate time-points detailed in Table S3 for the analysis of the kinetics of SLB- and SVL-formation. Larger arrows point the approximate times of the beginning and end of the vesicle injections.

QCM-Z experimental details

The average shifts in the normalized 3rd frequency overtone, along with the changes in energy dissipation, are presented in Figure S4. As in the SPR experiments, an additional step of injection of ultrapure H_2O was added subsequent to the vesicle injection for the DOPC-Sm-Chol mixture. Table S5 shows the final changes in overtone frequency, surface-mass density and energy dissipation for each lipid composition. For all cases, surface-mass densities were calculated using the Sauerbrey equation,

$$\Gamma = -C\frac{\Delta f_3}{3}, \qquad \text{(S3)}$$

where $C = 18.0\ \text{ng/cm}^2\text{Hz}$ for 4.95 MHz quartz crystal.

Table S5: Normalized QCM-Z frequency shifts from the 3rd overtone, surface-mass densities and energy dissipations for different SLBs. The values were calculated by averaging all the values after the injection of vesicles (DOPC, DOPC-DOPS, POPC, DPPC vesicles) and after the injection of ultrapure H_2O (DOPC-Sm-Chol).

	$\Delta f_{n,3}$ (Hz)	Γ_{QCM} (ng/cm^2)	ΔD (10^{-6})
DOPC	-24.21 ± 0.57	435.8 ± 10.3	0.46 ± 0.41
DOPC-DOPS	-25.85 ± 0.80	465.3 ± 14.4	0.59 ± 0.22
POPC	-26.04 ± 0.73	468.7 ± 13.1	0.31 ± 0.23
DOPC-Sm-Chol	-29.71 ± 0.61	534.8 ± 11.0	0.69 ± 0.11
DPPC vesicles	-221.6 ± 7.4	3989 ± 132	8.1 ± 3.0

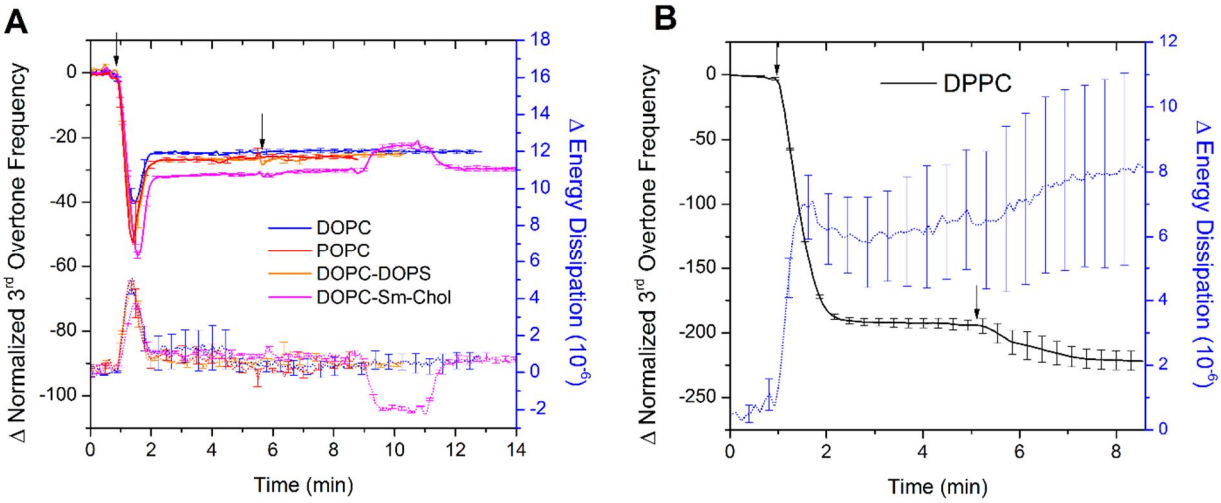

Figure S4: QCM-Z normalized frequency shifts at the 3rd overtone for A) SLB-forming vesicles and B) DPPC vesicles forming SVLs. Arrows point the approximate times of the beginning and end of the vesicle injections.

References

(1) LIPID Metabolites and Pathways Strategy (LIPID MAPS®) / Lipidomics Gateway http://www.lipidmaps.org/ 8.12.2017

(2) Mashaghi, A.; Swann, M.; Popplewell, J.; Textor, M.; Reimhult, E. Optical Anisotropy of Supported Lipid Structures Probed by Waveguide Spectroscopy and Its Application to Study of Supported Lipid Bilayer Formation Kinetics. Anal. Chem. 2008, 80 (10), 3666–3676.